ICSV 21
13-17 July, 2014, Beijing/China
The 21st International Congress on Sound and Vibration
13-17 July, 2014, Beijing/China

ESTIMATION OF RAILWAY VEHICLE SPEED USING GROUND VIBRATION MEASUREMENTS

Georges Kouroussis, Olivier Verlinden

Université de Mons – UMONS, Faculty of Engineering, 7000 Mons, Belgium
e-mail: georges.kouroussis@umons.ac.be

David P. Connolly

Heriot-Watt University, School of the Built Environment, Edinburgh EH14 4AS, Scotland

Mike C. Forde

University of Edinburgh, School of Engineering, Edinburgh EH9 3JF, Scotland

In railway noise and vibration assessment, the vehicle speed is a significant concern, since vehicle/track and track/soil interaction strongly affects the vibration magnitude. The objective of this paper is to analyse the dominant frequency method considered efficient in speed evaluation. Some enhancements are brought in order to extend the method applicability to a large speed range (tram, intercity train, high-speed train). For this purpose, a cepstral analysis was implemented to perform first speed estimation and a running rms was used to detect precisely the carbody passage excitation. A fitting is also achieved in order to efficiently improve the performance. Results coming from a railway–induced ground vibration prediction model allow validating the potential of the dominant frequency method and its stability. An application is proposed, based on recent measured high-speed train ground vibrations, in order to estimate with accuracy the associated vehicle speed.

1. Introduction

Various railway applications need the knowledge or, at least, an estimation of the vehicle speed. In railway-induced ground vibrations, it is well known that the train speed has a significant effect and its calculation is essential to correlate railway vibration levels [1–5]. Other applications are also concerned of knowing the vehicle speed. The use of vehicle tachometers is subject to some drawbacks: matching an exact speed to each track section, difficulty of communication with the rolling stock manager. Alternative methodologies for monitoring the train speed exist and have been applied with more or less success in the past. Let cite the use of a camera recorder (speed calculation based on the frames count) [3], the opposed photoelectric sensing method [6], or the time delay estimation with vibration sensors placed along the track. These applications need an access to the track with tedious installations or a track view access.

Regarding the use of vibrations sensors, Ni et al. [6] proposed an interesting method, called dominant frequency method, based on the isolation of dominant frequencies in the ground vibration spectrum. Indeed, the passing of axle load with periodicity generates significant peaks in the measured spectrum [7, 8]: at a specific location in the track, a train consists of a number of similar events with

certain delay times. Each peak is regularly spaced by

$$\Delta f_c = \frac{v_0}{L_c} \tag{1}$$

where v_0 is the vehicle speed (assumed to be constant during the recording) and L_c the carriage length of the studied vehicle (if the vehicle is composed of several different carriage length, L_c is equal to the most representative length, that's to say the length of the most usual carriage). Theoretically, a spectrum based on a sequence of the axles presents significant peaks in a large frequency band. In practice, ground vibrations generated by railway are complex, since the vehicle interacts with the track, and track and soil resonances can appears in the frequency range of interest. All these phenomena are illustrated in Tab. 1 which defines the typical excitation frequencies, according to [9–12]. Moreover, due to the limited vehicle speed (effect of the track deflection) and the foundation stiffness and damping, vibration magnitudes decrease with the frequency, limiting the dominant frequencies analysis.

Table 1. Main contribution of vehicle/track/soil properties on the ground vibration frequency content

Mechanisms	Equations	Typical frequencies
		0 50 100 150 200 f [Hz]
carriage spacing	$f_{c,n} = \frac{nv_0}{L_c}$	
sleeper spacing	$f_s = \frac{v_0}{L_s}$	
rail bending	$f_r = \frac{1}{2\pi}\sqrt{\frac{K_f}{\rho_r S_r}}$	
upper layer soil	$f_{soil} = \frac{c_p}{4h}$	
vehicle dynamics		

The dominant frequency method proposed by Ni et al. [6] takes partially into account these interferences. It utilises an automatic procedure which evaluates each carriage excitation frequency from the spectra amplitude $V_i(f)$ of measured ground vibrations $v_i(t)$ at a specified distance from the track and along any one of the three directions ($i = x$, y or z for horizontal parallel to the track, horizontal perpendicular to the track or vertical, respectively). The calculation starts from a frequency range specified by the user, within which the fundamental frequency is found at maximum amplitude. Then a recursive calculation of the harmonic dominant frequencies are performed by finding the maximum in the frequency range calculated from an average excitation frequency, obtained from the previously calculated excitation frequencies. A speed is then estimated for each harmonic excitation frequency with the help of Eq. (1) and a minimum difference criterion is applied for determining the train speed. The authors validated their method by calculating high-speed train (HST) passage speeds, verified using experimental results from optical sensors, for speeds in the range 200–$300\,\mathrm{km/h}$.

This paper investigates the dominant frequency method and proposes improvements in order to extend its domain of validity. Indeed, several shortcomings are pointed out in the present work: a poor estimation of fundamental dominant excitation frequency can prevent divergence in the calculation of vehicle speed and the calculation of each harmonic can be subject to errors if the signal contains strong excitations from sources other than from the vehicle periodicity (e.g. vehicle natural frequency or soil resonance). Two new methods have been developed in order to prevent these negative points, and are combined into a single approach with the original dominant frequency method. In order to demonstrate the effectiveness of the new method and to show its ability to predict a wide spectrum

of train speeds, practical results are presented, coming from numerical results for which the vehicle speed is known and from experimental measurements established in the past.

2. Train speed calculation technique

The newly proposed procedure is summarized in Figure 1 where a focus on the enhancements is made over the original dominant frequency method. The calculation technique is defined in three steps where an initial speed is required, and is summarized as follow.

- In order to better estimate the fundamental dominant excitation frequency, a cepstral analysis is applied to the vibration signal spectrum:

$$C_v(\tau) = \mathrm{iDFT}\left(\log\left|V_i(f)\right|\right) \ . \tag{2}$$

  This operation is able to reveal and quantify f_c (the carriage excitation frequency) but also f_a (the wheelset excitation frequency) and f_b (the bogie excitation frequency). All these values are dependant of the vehicle speed and the main vehicle geometry.

- The use of the dominant frequency method is based on the running rms instead of the original signal

$$v_{rms,\tau}(t_0) = \sqrt{\frac{1}{\tau}\int_{t_0-\tau}^{t_0} v_i^2(t) e^{\frac{t-t_0}{\tau}} \mathrm{d}t} \ . \tag{3}$$

  This allows a clearer visualization of passing of each wheelset.

- To avoid limitations due to the signal frequency resolution and the other sources excitations, a regression analysis is performed which combines the ground vibration measurements with analytical solution to update the vehicle speed parameter. A simple formulation is used for the fitting, based on rules for time-delayed Dirac functions:

$$V^{analytical}(f) = A\mathrm{e}^{-\alpha f}\left|\left(1+\mathrm{e}^{-j2\pi f/f_a}\right)\left(1+\mathrm{e}^{-j2\pi f/f_b}\right)\left(1+\sum_{i=1}^{n_c}\mathrm{e}^{-j2\pi i f/f_c}\right)\right| \tag{4}$$

  where n_c is the number of carriages and A and α the fitted amplitude and decay rate, respectively.

If multiple ground vibration signals are used, an average analysis is performed to estimate the speed mean v_0 from all sensors after each step. Additional details related to its development are available in [13, 14].

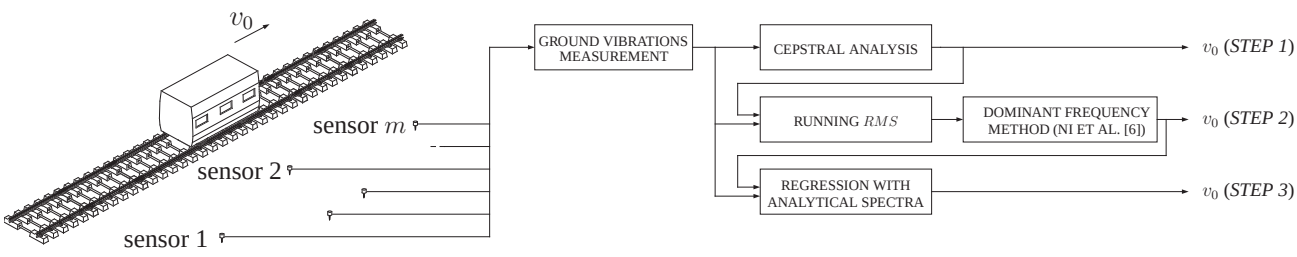

Figure 1. Chart of the automatic procedure for estimating the vehicle speed

3. Results

3.1 Numerical ground vibrations: validation

The validation is performed using a numerical prediction model for speed calculation validation. It allows for a high accuracy comparison because the vehicle speed is known and a wide variety of train types, speeds and soil conditions can be tested. This section presents the analysis of the Thalys HST. Figure 2 presents the main train dimensions, showing that the central carriages are equipped to non-conventional bogies (Jacob's bogie). It is important that the new method is able to predict speeds for both high and low velocity trains. Therefore different speeds are analysed in order to determine its influence on the speed estimates.

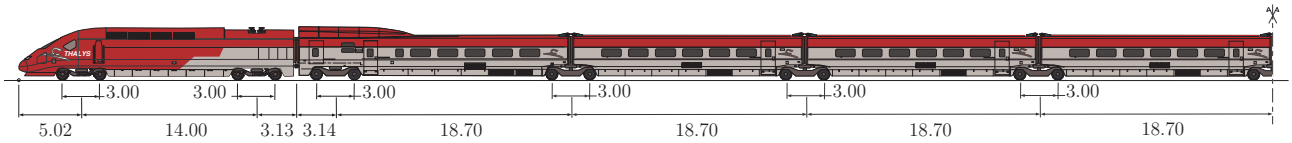

Figure 2. Thalys HST dimensions

To illustrate the frequency range of excitation, Figure 3 presents the frequency spectra of the ballast vertical reaction. With the speed, each peak is located along a line with slope proportional to speed. Furthermore, it displays the fundamental ($n = 1$) and the harmonics ($n > 1$) of the carbody passage frequency directly in the excitation spectrum and as a function of the vehicle speed. Some peaks exhibit high amplitudes (e.g. $n = 1$ or 5) while others are almost completely suppressed ($n = 3$), due to the sidebands generated by the axle passage frequency. Overall, a decrease in amplitude with increasing frequency is also observable. These observations can be used to estimate vehicle speed and to valid the method robustness.

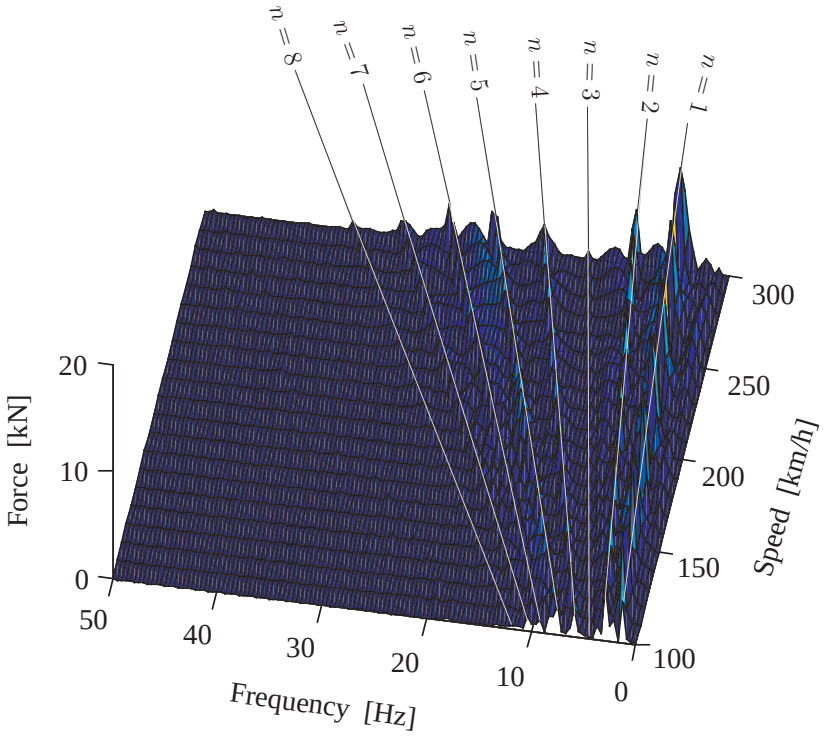

Figure 3. Spectral content of the soil loading as a function of the HST speed

Figure 4 displays the relative error at each step of the evaluation. Clearly, the final speed calculated using the analytical model and regression yields the most accurate estimate. The cepstral

analysis is also accurate, but for several speeds, the error is large. No notable influence of the magnitude of speed is observed in the results.

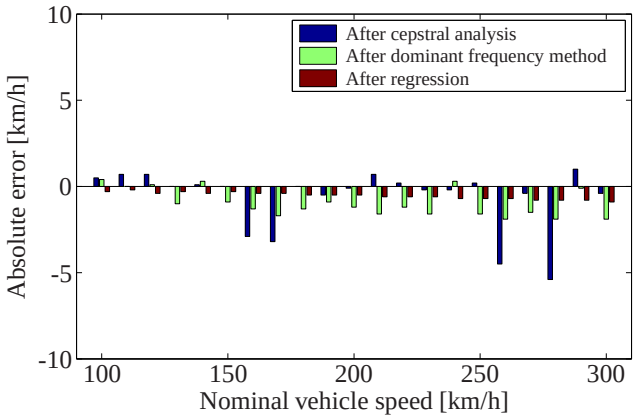

Figure 4. Evaluation differences of the dominant frequency method for the Thalys HST as a function of the speed

3.2 Field trials performed on operational railway lines

For this purpose, the train speed calculator was used to predict train speeds collected by [3]. In this work, experimental results were used to validate the aforementioned ground vibration prediction model near the high-speed line LGV1 between Brussels and Paris/London. Sensors were placed from 3 to $43\,\mathrm{m}$ from the external side of closest track. Train passages in both track directions were measured.

Five-teen train passages were recorded (12 Thalys, 2 Eurostar HST and 1 French TGV). The Eurostar TransManche super train (Fig. 5) had the same configuration as the Thalys HST, except in the centre where two side carriages are added for safety reasons related to tunnel passage. Its length was nearly twice than the Thalys with a total dimension of $394\,\mathrm{m}$. The French TGV is currently the forerunner HST and mainly circulates in France. It has the same dimensions as the Thalys (Fig. 2). It should be mentioned that "Thalys double" passages were also recorded. These consisted of two single Thalys trains hooked up in series.

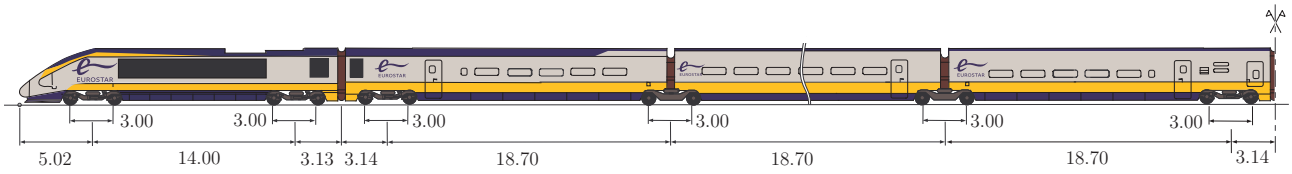

Figure 5. Eurostar HST dimensions

During these tests, train speed was originally estimated using two methods: using a camera and using an additional vibration sensors placed along the track (time delay estimator). Table 2 lists each passage and notes the original estimated speed (penultimate column). The final column gives the vehicle speed calculated by the present method. Overall a good agreement is observed, except for a few trains which exhibit a slightly greater error (less than $10\,\%$). These inconsistent initial estimations do not affect the conclusions drawn in [3], because a low dependency of the train speed on the vibration level was observed.

More recently, Connolly performed a similar experimental analysis for the purpose of analysing the effect of embankment conditions on high speed rail ground vibrations in UK. A set of sensors have been placed along a profile perpendicular to the track in order to estimate the generated ground vibrations, similarly to the preceding study. High Speed 1 (HS1), linking London, UK and Paris,

Table 2. Speed evaluation during the passing of HST's [3]

Name	Train code	Time	Train type	Track	# carriages	Nominal speed [km/h]	Calculated speed [km/h]
ThalysB1	9327	12:33	Thalys	B	8	305	291.9
ThalysA1	9326	12:35	Thalys	A	8	295	301.8
ThalysB2	9429	12:57	Thalys	B	8	300	298.9
ThalysA2	9428	12:58	Thalys	A	8	275	300.2
ThalysA3	9960	13:14	Thalys	A	2×8	270	293.2
EurostarA1	9133	13:18	Eurostar	A	18	280	298.9
ThalysA4	9330	13:29	Thalys	A	8	265	288.4
ThalysB3	9331	13:30	Thalys	B	8	285	285.3
ThalysB4	9927	13:38	Thalys	B	8	250	258.5
EurostarB1	9124	13:46	Eurostar	B	18	290	296.9
ThalysB5	9333	13:58	Thalys	B	2×8	295	297.4
ThalysA5	9436	15:00	Thalys	A	8	260	283.8
ThalysA6	9338	15:28	Thalys	A	8	265	282.7
ThalysB6	9339	15:30	Thalys	B	8	305	302.0
TGVfnA1	9832	15:35	TGV	A	8	270	292.4

France via the Channel Tunnel beneath the English Channel, has been investigated. Passages of Eurostar and Javelin HST's were recorded on 25^{th} September 2012 – 27^{th} September 2012 at three test sites close to Hollingbourne, UK. Site 1 was an at-grade section, site 2 on top of a tunnel, and site 3 on an embankment. Site 1 had a cutting on one side and at-grade on other side. Tests were performed on the at-grade side. Site 2 was situated above a "cut and cover" tunnel. Site 3 was on an embankment.

The Javelin Class 395 is an electric multiple unit built in Japan by Hitachi for high speed commuter services on HS1. It is capable of running at a maximum speed of $225\,\text{km/h}$ under overhead electrification on HS1, and $161\,\text{km/h}$ on 750V DC third rail supply on conventional lines. Similarly to Thalys trains, two Javelings can be linked together. Therefore the basic 6-carriage train can be adapted to create a 12-carriage system. Javelin class 395 trains are composed of intercity train carriages that have been upgraded to facilitate elevated speeds. Therefore more conventional bogies are used (for all carriages) in comparison to dedicated high speed bogies found in Thalys, TGV and Eurostar trains (Fig. 6). Unlike the aforementioned high speed trains, the Javelin carriage spacing ($L_c = 20\text{m}$) is greater than the bogie spacing ($L_b = 14.17\,\text{m}$). Therefore the excitation frequencies associated with L_b and L_c are different. Tables 3 to 5 list the different passages recorded and the calculated vehicle speed.

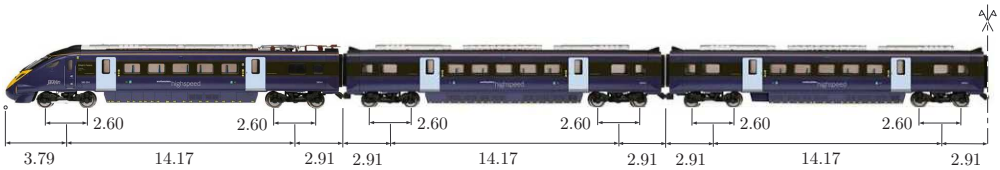

Figure 6. Javelin 395 HST dimensions

4. Conclusions

Similarly to the use of vibrations with the aim to generate electrical power (on high-speed road or in dance club), the vibrations generated by the passing of train can be seen as an opportunity to

Table 3. Speed evaluation during the passing of HST's on the high speed line HS1 in UK (at-grade track configuration)

Recorded train	Track	Time	Speed [km/h]
Eurostar	A	12:09	261.3
Javelin 395	B	12:10	220.4
Javelin 395	B	12:42	216.2
Javelin 395	A	12:51	223.3
Eurostar	A	12:52	285.2
Eurostar	A	13:11	289.0
Javelin 395	A	13:21	223.2
Eurostar	A	13:25	287.7
Eurostar	A	13:41	298.2

Table 4. Speed evaluation during the passing of HST's on the high speed line HS1 in UK (above the tunnel)

Recorded train	Track	Time	Speed [km/h]
Eurostar	A	?	265.5
Javelin 395	A	12:11	206.7

Table 5. Speed evaluation during the passing of HST's on the high speed line HS1 in UK (embankment track configuration)

Recorded train	Track	Time	Speed [km/h]
Javelin 395	A	12:10	204.2
Javelin 395	B	12:30	197.5
Eurostar	B	12:36	289.6
Eurostar	A	12:52	283.3
Javelin 395	B	12:52	198.1
Javelin 395	A	13:10	206.5
Eurostar	B	13:11	291.1
Eurostar	A	13:23	288.0
Javelin 395	B	13:30	198.3
Eurostar	B	13:40	268.5

capture the train speed. Based on the dominant frequency method, a newly tool is presented in this paper, enhancing the original method and filling its drawbacks. Various signal processing procedures are implemented in order to offer a semi-remote, non-invasive and economical method for vehicle speed monitoring. In the case of ground vibration measurement, no additional device is needed.

To show the robustness and ability of the proposed method to calculate a wide range of train speeds, it is used to predict speeds from numerically generated train passages. The method is then applied to measured results in order to complete an experimental database useful for further numerical prediction model validation. Moreover, its applicability for various track configurations (embankment, cutting, tunnel) is shown.

Acknowledgement

The first author would like to acknowledge, C. Crémer, A. Mégret, M. Courtois and T. Hoet, from the Faculty of Engineering of the University of Mons, for their investigations into the dominant

frequency method applicability.

REFERENCES

[1] U. S. Department of Transportation (Federal Railroad Administration). High-speed ground transportation. Noise and vibration impact assessment. Technical Report 293630–1, Office of Railroad Development Washington, 1998.

[2] G. Degrande and L. Schillemans. Free field vibrations during the passage of a Thalys high-speed train at variable speed. *Journal of Sound and Vibration*, 247(1):131–144, 2001.

[3] G. Kouroussis, O. Verlinden, and C. Conti. Free field vibrations caused by high-speed lines: measurement and time domain simulation. *Soil Dynamics and Earthquake Engineering*, 31(4):692–707, 2011.

[4] D. Connolly, A. Giannopoulos, and M. Forde. Numerical modelling of ground borne vibrations from high speed rail lines on embankments. *Soil Dynamics and Earthquake Engineering*, 46:13–19, 2013.

[5] D. P. Connolly, G. Kouroussis, A. Giannopoulos, O. Verlinden, P. K. Woodward, and M. C. Forde. Assessment of railway vibrations using an efficient scoping model. *Soil Dynamics and Earthquake Engineering*, 58:37–47, 2014.

[6] S.-H. Ni, Y.-H. Huang, and K.-F. Lo. An automatic procedure for train speed evaluation by the dominant frequency method. *Computers and Geotechnics*, 38(4):416–422, 2011.

[7] L. Auersch. Ground vibration due to railway traffic — the calculation of the effects of moving static loads and their experimental verification. *Journal of Sound and Vibration*, 293(3–5):599–610, 2006.

[8] S.-H. Ju, H.-T. Lin, and J.-Y. Huang. Dominant frequencies of train-induced vibrations. *Journal of Sound and Vibration*, 319(1-2):247–259, 2009.

[9] M. Heckl, G. Hauck, and R. Wettschureck. Structure-borne sound and vibration from rail traffic. *Journal of Sound and Vibration*, 193(1):175–184, 1996.

[10] G. Lefeuve-Mesgouez, A. T. Peplow, and D. Le Houédec. Surface vibration due to a sequence of high speed moving harmonic rectangular loads. *Soil Dynamics and Earthquake Engineering*, 22(6):459–473, 2002.

[11] T. Dahlberg. Railway track dynamics — a survey. Technical Report Railtrdy.doc/2003-11-06/td, Linköping University, 2003.

[12] G. Kouroussis, O. Verlinden, and C. Conti. Influence of some vehicle and track parameters on the environmental vibrations induced by railway traffic. *Vehicle System Dynamics*, 50(4):619–639, 2012.

[13] G. Kouroussis, D. P. Connolly, M. C. Forde, and O. Verlinden. Estimation of the railway rolling stock speed from free field ground vibrations measurement. In *Transportation Research Board 93rd Annual Meeting*, Washington (USA), 2014.

[14] G. Kouroussis, D. P. Connolly, M. C. Forde, and O. Verlinden. Train speed calculation using ground vibrations. *Proceedings of the Institution of Mechanical Engineers, Proc. IMechE Part F: Journal of Rail and Rapid Transit*, doi: 10.1177/0954409713515649.